www.ietdl.org

Published in IET Systems Biology
Received on 4th January 2011
Revised on 17th May 2011
doi: 10.1049/iet-syb.2011.0001

ISSN 1751-8849

Qualitative modelling and formal verification of the FLR1 gene mancozeb response in *Saccharomyces cerevisiae*

P.T. Monteiro[1,2] *P.J. Dias*[3,4] *D. Ropers*[2] *A.L. Oliveira*[1] *I. Sá-Correia*[3,4] *M.C. Teixeira*[3,4] *A.T. Freitas*[1]

[1]*INESC-ID/IST, Rua Alves Redol 9, Lisboa 1000-029, Portugal*
[2]*INRIA Grenoble – Rhône-Alpes, 655 Avenue de l'Europe, Montbonnot, St. Ismier Cedex 38334, France*
[3]*Department of Bioengineering, Instituto Superior Técnico, Technical University of Lisbon, 1049-001 Lisboa, Portugal*
[4]*IBB – Institute for Biotechnology and Bioengineering, CEBQ-IST, 1049-001 Lisboa, Portugal*
E-mail: ptgm@kdbio.inesc-id.pt

Abstract: *Background:* Qualitative models allow understanding the relation between the structure and the dynamics of gene regulatory networks. The dynamical properties of these models can be automatically analysed by means of formal verification methods, like model checking. This facilitates the model-validation process and the test of new hypotheses to reconcile model predictions with the experimental data. *Results:* The authors report in this study the qualitative modelling and simulation of the transcriptional regulatory network controlling the response of the model eukaryote *Saccharomyces cerevisiae* to the agricultural fungicide mancozeb. The model allowed the analysis of the regulation level and activity of the components of the gene mancozeb-induced network controlling the transcriptional activation of the FLR1 gene, which is proposed to confer multidrug resistance through its putative role as a drug efflux pump. Formal verification analysis of the network allowed us to confront model predictions with the experimental data and to assess the model robustness to parameter ordering and gene deletion. *Conclusions:* This analysis enabled us to better understand the mechanisms regulating the FLR1 gene mancozeb response and confirmed the need of a new transcription factor for the full transcriptional activation of YAP1. The result is a computable model of the FLR1 gene response to mancozeb, permitting a quick and cost-effective test of hypotheses prior to experimental validation.

1 Background

Modern experimental techniques have yielded large amounts of biological regulatory data. However, the understanding of how specific structural interactions between molecular components influence the global behaviour of a biological regulatory network is still not completely understood. This has motivated the use of formal models in order to capture dynamical behaviours of the corresponding biological processes [1–9]. Despite the increasing amount of biological data, precise quantitative information is generally not available for the tuning of the model parameter values. The use of qualitative models is thus appropriate to capture the available information, focusing mainly on the evolution trends rather than on the precise quantitative values [1, 10–14].

In this study, we analyse the regulation of the transcriptional activation of the FLR1 gene in yeast cells exposed to the agricultural fungicide mancozeb, by means of a mathematical model and formal verification techniques. The FLR1 gene encodes a plasma membrane member of the 12-spanner Drug:H^+ Antiporter DHA1 family of the Major Facilitator Superfamily, involved in the multidrug resistance phenomenon [15–18], and proposed to catalyse the extrusion of toxic compounds, including mancozeb [15]. Although *Saccharomyces cerevisiae* is not a phytopathogen, results obtained in this model eukaryote are expected to have a parallel in mancozeb-targeted organisms [19] for the study of fungicide resistance.

In the previous study [20], we have built a network composed of four known transcription factors regulating the transcriptional activation of the FLR1 gene: Yap1, Yrr1, Rpn4 and Pdr3 (Fig. 1). The transcriptional activation of FLR1 in yeast cells exposed to mancozeb is completely dependent on the Yap1 transcription factor [15]. However, to obtain full activation of the FLR1 gene, Yrr1, Pdr3 and Rpn4 are also required [15]. Furthermore, the effect of Yap1, Yrr1 and Pdr3 in FLR1 transcription is known to be direct, as proven by in vivo Chromatine ImmunoPrecipitation (ChIP) [21, 22] or promoter site-directed mutagenesis (see [20] for a full description of the network interactions). In this work, we analyse the role of these factors in the adjustment of the concentration of Flr1 protein following mancozeb addition by means of a mathematical model.

The current unavailability of precise kinetic parameters and molecular concentrations motivated the use of a qualitative modelling framework. Examples of such formalisms are Boolean or other logical models [10–12] and Petri nets [1, 13, 14]. However, the analysis of the dynamical behaviour

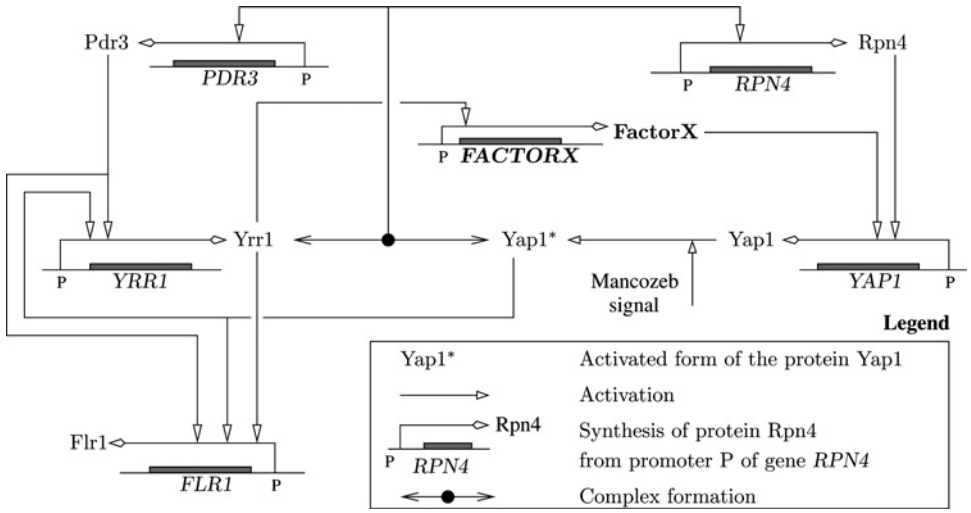

Fig. 1 *Network of key genes, proteins and regulatory interactions involved in the FLR1 response to the presence of mancozeb in S. cerevisiae*

of the networks from the models, yields large amounts of predictions that need to be manually verified against experimental data, which quickly becomes infeasible as the size of the models grows.

Methods from the field of formal verification provide a promising way to deal with the analysis of large and complex models [23]. Model checking, the method selected for this study, uses specific algorithms to automatically and exhaustively search the state space and verify whether dynamical properties, encoded as statements in temporal logic, are satisfied or not by the model [24]. Despite the presence of several examples in the literature of the application of model checking to the analysis of biological models [1–9], only recently that some of the obstacles impeding its widespread application were addressed [25].

This work proposes a computable model to describe the FLR1 gene response network activated in the presence of the fungicide mancozeb in *S. cerevisiae* cells. The model was analysed using the genetic network analyser (GNA) modelling and simulation tool [26], through an iterative process where, at each step, the models predictions were compared with the available experimental data. The model was also perturbed to assess the robustness of the built network by performing single and double knockouts, obtaining the resulting mancozeb response steady states and comparing them with the available experimental data for single and double mutants [15, 20]. This analysis provided us not only with a model that could explain most of the available data, but also evidenced the necessity for the inclusion of a new transcription factor in the network to account for the remainder.

2 Results

To model the FLR1 regulatory network, we considered previous knowledge on the transcriptional profile of each of the variables of the network registered upon exposure to the fungicide mancozeb and obtained by quantitative RT-PCR [15, 20]. These variables include, besides FLR1 itself, five transcription factors: Yap1, known to control oxidative stress response, Pdr3 and Yrr1, two regulators of multidrug resistance in yeast, Rpn4, known to control the expression of proteasome genes, required to intensify protein degradation under stress, and a fifth transcription factor, added to the network for reasons that will be described below.

2.1 Qualitative modelling of the FLR1 gene mancozeb response network

This section describes the translation of the FLR1 gene mancozeb response network into a kinetic model. The objective is to obtain a model able to predict changes in the concentrations of the network proteins following mancozeb addition, which can be directly confronted to the experimental data in [15]. In the absence of detailed information on the molecular interactions, we use piecewise-linear (PL) differential equations to describe the rate of change of protein concentrations. This qualitative modelling framework, originally introduced by Glass and Kauffman [27], provides a coarse-grained description of the network dynamics, in the sense that it does not explicitly specify the biochemical mechanisms. The qualitative dynamics of PL models is relatively simple to analyse, using inequality constraints on the parameters rather than exact numerical values (see Section 5). PL models are generally good approximations of ordinary differential equations (ODE) models, even in the case of large biochemical networks [28, 29]. They can also be used as a first step to orient the development of more detailed quantitative ODE models.

2.1.1 General form of the FLR1 network model: We introduce six state variables, each corresponding to the total concentration of a protein for a given gene, and one input variable denoting the mancozeb concentration (Table 1). The time derivative of each variable equals the difference between the rate of protein synthesis and the rate of protein degradation.

The PL model has the general form

$$\dot{x}_i = \sum_{l \in L_i} \kappa_i^l s_i^l(x) - \gamma_i x_i, \quad x_i \geq 0, \quad 1 \leq i \leq n$$

where $\boldsymbol{x} = (x_1, \ldots, x_n)'$ is a vector of protein concentrations. The synthesis rate is a sum of synthesis constants κ_i^l, each modulated by a regulation function $s_i^l(x)$ taking the values $\{0, 1\}$, with L_i a possibly empty set of indices of regulation functions. We notably define a basal synthesis constant κ_i^b for each variable to account for protein expression in the absence of mancozeb and up to three synthesis constants for the regulation of gene expression by mancozeb and

Table 1 FLR1 gene mancozeb response network in *S. cerevisiae*

$$\dot{u}_{\text{mancozeb}} = 0$$
$$0 < \theta_{\text{mancozeb}} < \max_{\text{mancozeb}}$$

$$\dot{x}_{\text{flr1}} = \kappa^{b}_{\text{flr1}} + \kappa^{1}_{\text{flr1}} s^{+}(x_{\text{yap1}}, \theta^{1}_{\text{yap1}}) s^{+}(u_{\text{mancozeb}}, \theta_{\text{mancozeb}}) + \kappa^{2}_{\text{flr1}}\, s^{+}(x_{\text{pdr3}}, \theta^{1}_{\text{pdr3}})\, s^{+}(x_{\text{yap1}}, \theta^{1}_{\text{yap1}})\, s^{+}(u_{\text{mancozeb}}, \theta_{\text{mancozeb}}) + \kappa^{3}_{\text{flr1}} s^{+}(x_{\text{yrr1}}, \theta^{2}_{\text{yrr1}}) s^{+}(x_{\text{yap1}}, \theta^{3}_{\text{yap1}}) s^{+}(u_{\text{mancozeb}}, \theta_{\text{mancozeb}}) - \gamma_{\text{flr1}}\, x_{\text{flr1}}$$

$$0 < \kappa^{b}_{\text{flr1}}/\gamma_{\text{flr1}} < (\kappa^{b}_{\text{flr1}} + \kappa^{1}_{\text{flr1}})/\gamma_{\text{flr1}} < (\kappa^{b}_{\text{flr1}} + \kappa^{2}_{\text{flr1}})/\gamma_{\text{flr1}} < (\kappa^{b}_{\text{flr1}} + \kappa^{1}_{\text{flr1}} + \kappa^{2}_{\text{flr1}})/\gamma_{\text{flr1}} < (\kappa^{b}_{\text{flr1}} + \kappa^{3}_{\text{flr1}})/\gamma_{\text{flr1}} < (\kappa^{b}_{\text{flr1}} + \kappa^{1}_{\text{flr1}} + \kappa^{3}_{\text{flr1}})/\gamma_{\text{flr1}} < (\kappa^{b}_{\text{flr1}} + \kappa^{2}_{\text{flr1}} + \kappa^{3}_{\text{flr1}})/\gamma_{\text{flr1}} < (\kappa^{b}_{\text{flr1}} + \kappa^{1}_{\text{flr1}} + \kappa^{2}_{\text{flr1}} + \kappa^{3}_{\text{flr1}})/\gamma_{\text{flr1}} < \max_{\text{flr1}}$$

$$\dot{x}_{\text{pdr3}} = \kappa^{b}_{\text{pdr3}} + \kappa^{1}_{\text{pdr3}}\, s^{+}(x_{\text{yrr1}}, \theta^{1}_{\text{yrr1}})\, s^{+}(x_{\text{yap1}}, \theta^{1}_{\text{yap1}})\, s^{+}(u_{\text{mancozeb}}, \theta_{\text{mancozeb}}) - \gamma_{\text{pdr3}}\, x_{\text{pdr3}}$$

$$0 < \kappa^{b}_{\text{pdr3}}/\gamma_{\text{pdr3}} < \theta^{1}_{\text{pdr3}} < (\kappa^{b}_{\text{pdr3}} + \kappa^{1}_{\text{pdr3}})/\gamma_{\text{pdr3}} < \max_{\text{pdr3}}$$

$$\dot{x}_{\text{yrr1}} = \kappa^{b}_{\text{yrr1}} + \kappa^{1}_{\text{yrr1}}\, s^{+}(x_{\text{yap1}}, \theta^{b}_{\text{yap1}})\, s^{+}(u_{\text{mancozeb}}, \theta_{\text{mancozeb}}) + \kappa^{2}_{\text{yrr1}}\, s^{+}(x_{\text{pdr3}}, \theta^{1}_{\text{pdr3}}) + \kappa^{3}_{\text{yrr1}}\, s^{+}(x_{\text{yap1}}, \theta^{3}_{\text{yap1}})\, s^{+}(u_{\text{mancozeb}}, \theta_{\text{mancozeb}}) - \gamma_{\text{yrr1}}\, x_{\text{yrr1}}$$

$$0 < \kappa^{b}_{\text{yrr1}}/\gamma_{\text{yrr1}} < \theta^{1}_{\text{yrr1}} < (\kappa^{b}_{\text{yrr1}} + \kappa^{1}_{\text{yrr1}})/\gamma_{\text{yrr1}} < \theta^{2}_{\text{yrr1}} < (\kappa^{b}_{\text{yrr1}} + \kappa^{2}_{\text{yrr1}})/\gamma_{\text{yrr1}} < (\kappa^{b}_{\text{yrr1}} + \kappa^{1}_{\text{yrr1}} + \kappa^{2}_{\text{yrr1}})/\gamma_{\text{yrr1}} < \theta^{3}_{\text{yrr1}} < (\kappa^{b}_{\text{yrr1}} + \kappa^{3}_{\text{yrr1}})/\gamma_{\text{yrr1}} < (\kappa^{b}_{\text{yrr1}} + \kappa^{1}_{\text{yrr1}} + \kappa^{3}_{\text{yrr1}})/\gamma_{\text{yrr1}} < (\kappa^{b}_{\text{yrr1}} + \kappa^{2}_{\text{yrr1}} + \kappa^{3}_{\text{yrr1}})/\gamma_{\text{yrr1}} < (\kappa^{b}_{\text{yrr1}} + \kappa^{1}_{\text{yrr1}} + \kappa^{2}_{\text{yrr1}} + \kappa^{3}_{\text{yrr1}})/\gamma_{\text{yrr1}} < \max_{\text{yrr1}}$$

$$\dot{x}_{\text{rpn4}} = \kappa^{b}_{\text{rpn4}} + \kappa^{1}_{\text{rpn4}}\, s^{+}(x_{\text{yrr1}}, \theta^{1}_{\text{yrr1}})\, s^{+}(x_{\text{yap1}}, \theta^{1}_{\text{yap1}})\, s^{+}(u_{\text{mancozeb}}, \theta_{\text{mancozeb}}) - \gamma_{\text{rpn4}}\, x_{\text{rpn4}}$$

$$0 < \kappa^{b}_{\text{rpn4}}/\gamma_{\text{rpn4}} < \theta^{1}_{\text{rpn4}} < (\kappa^{b}_{\text{rpn4}} + \kappa^{1}_{\text{rpn4}})/\gamma_{\text{rpn4}} < \max_{\text{rpn4}}$$

$$\dot{x}_{\text{yap1}} = \kappa^{b}_{\text{yap1}} + \kappa^{1}_{\text{yap1}}\, s^{+}(u_{\text{mancozeb}}, \theta_{\text{mancozeb}}) + \kappa^{2}_{\text{yap1}}\, s^{+}(x_{\text{rpn4}}, \theta^{1}_{\text{rpn4}}) + \kappa^{3}_{\text{yap1}}\, s^{+}(x_{\text{factorX}}, \theta^{1}_{\text{factorX}}) - \gamma_{\text{yap1}}\, x_{\text{yap1}}$$

$$0 < \kappa^{b}_{\text{yap1}}/\gamma_{\text{yap1}} < \theta^{1}_{\text{yap1}} < (\kappa^{b}_{\text{yap1}} + \kappa^{1}_{\text{yap1}})/\gamma_{\text{yap1}} < (\kappa^{b}_{\text{yap1}} + \kappa^{2}_{\text{yap1}})/\gamma_{\text{yap1}} < (\kappa^{b}_{\text{yap1}} + \kappa^{1}_{\text{yap1}} + \kappa^{2}_{\text{yap1}})/\gamma_{\text{yap1}} < \theta^{2}_{\text{yap1}} < (\kappa^{b}_{\text{yap1}} + \kappa^{3}_{\text{yap1}})/\gamma_{\text{yap1}} < (\kappa^{b}_{\text{yap1}} + \kappa^{1}_{\text{yap1}} + \kappa^{3}_{\text{yap1}})/\gamma_{\text{yap1}} < (\kappa^{b}_{\text{yap1}} + \kappa^{2}_{\text{yap1}} + \kappa^{3}_{\text{yap1}})/\gamma_{\text{yap1}} < \theta^{3}_{\text{yap1}} < (\kappa^{b}_{\text{yap1}} + \kappa^{1}_{\text{yap1}} + \kappa^{2}_{\text{yap1}} + \kappa^{3}_{\text{yap1}})/\gamma_{\text{yap1}} < \max_{\text{yap1}}$$

$$\dot{x}_{\text{factorX}} = \kappa^{b}_{\text{factorX}} + \kappa^{1}_{\text{factorX}}\, s^{+}(x_{\text{yrr1}}, \theta^{1}_{\text{yrr1}})\, s^{+}(u_{\text{mancozeb}}, \theta_{\text{mancozeb}}) - \gamma_{\text{factorX}}\, x_{\text{factorX}}$$

$$0 < \kappa^{b}_{\text{factorX}}/\gamma_{\text{factorX}} < \theta^{1}_{\text{factorX}} < (\kappa^{b}_{\text{factorX}} + \kappa^{1}_{\text{factorX}})/\gamma_{\text{factorX}} < \max_{\text{factorX}}$$

Model has six state variables corresponding to the concentrations of the transcription factors and the regulated FLR1 gene, as well as one input variable denoting the presence of the fungicide mancozeb in the cell

other transcription factors. The degradation of each protein is a first-order term with a degradation constant γ_i, since no regulation of protein stability has been evidenced for the network proteins. A regulation function is an algebraic expression of step functions $s^{+}(x_i, \theta_i)$, which formalises the regulatory logic of gene expression. θ_i is a threshold for the concentration x_j. The step function $s^{+}(x_i, \theta_i)$ evaluates to 1 if $x_i > \theta_i$, and to 0 if $x_i < \theta_i$, thus capturing the switch-like character of gene regulation.

Note that transcription and translation are lumped in one single step in our model. Indeed, changes in mRNA and protein levels are considered to be correlated, since the effect of mancozeb addition occurs mainly at the transcriptional level [15]. Therefore we directly compare the predicted protein concentrations to the mRNA levels monitored in [15], similarly to the approximation made by Cantone *et al.* [30].

2.1.2 Modelling of interactions in the FLR1 network

2.1.2.1 Transcriptional activator: The regulatory mechanism of the YAP1 activation by Rpn4 depicted in Fig. 2*a* can be represented by the sigmoidal Hill function, commonly used to capture the cooperative effects experimentally observed for the control of protein synthesis (see Section 7 for the modelling details and Fig. 2*b*). Below a certain threshold value of Rpn4, YAP1 is poorly expressed, whereas above this threshold its expression reaches its maximum level. The Hill function can be approximated by a step function, as shown in Fig. 2*b*, yielding the following rate of expression

$$f_{\text{yap1}}(x_{\text{rpn4}}) = \kappa^{2}_{\text{yap1}} s^{+}(x_{\text{rpn4}}, \theta^{1}_{\text{rpn4}})$$

The function $f_{\text{yap1}}(x_{\text{rpn4}})$ implies that YAP1 is expressed at a rate of κ^{2}_{yap1} if Rpn4 is above its threshold concentration and it is not expressed otherwise. We apply the same reasoning to describe other direct interactions in the network, notably transcriptional activation by Yap1, FactorX and mancozeb.

2.1.2.2 Transcriptional regulator activated by mancozeb: The derivation of step-function expressions is less trivial when the network interactions are indirect. Consider, for instance, the activation of Pdr3 transcription by the complex

doi: 10.1049/iet-syb.2011.0001

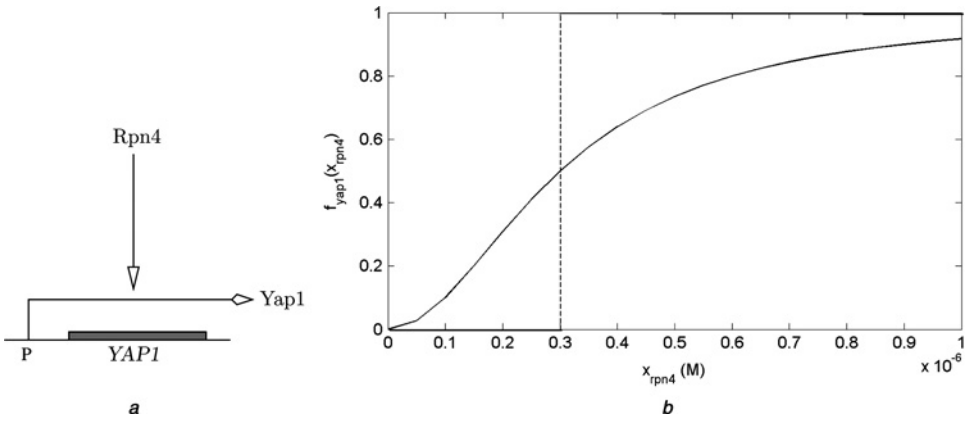

Fig. 2 *Transcriptional activator*

a Regulation of YAP1 expression by the protein Rpn4
b Activity of the YAP1 promoter as a function of Rpn4 concentration (see Methods). The Hill function is approximated by a step function, which changes its value from 0 to 1 at a threshold concentration of Rpn4

Yrr1 − Yap1*, which is formed in response to mancozeb stress (Fig. 3*a*). Following its sensing by yeast cells through still unknown mechanisms, mancozeb activates transcription factors at the transcriptional [15] and post-translational levels. For instance, Yap1 is activated by the formation of intra-molecular disulfide bonds in the presence of oxidants, alkylating or thiol-reactive agents. The activated form of the protein, Yap1*, is preferentially targeted to the nucleus [31], where it binds to Yrr1 and regulates gene expression. We therefore describe the regulation of the PDR3 synthesis rate by Yrr1 and Yap1 in the presence of mancozeb, through their effect on Yrr1 − Yap1* concentration.

We have developed a kinetic model for the above regulatory mechanism, using mass-action and Hill rate laws, as well as plausible parameter values derived from the literature (see Section 7 for details). The resulting model has been used to calculate the activity of promoter PDR3 as a function of the total Yrr1 and Yap1 concentrations, in the presence and absence of mancozeb. There is no PDR3 up-regulation in the absence of mancozeb, while the response function is sigmoidal when mancozeb is present (Fig. 3*b*).

The sigmoidal surface in Fig. 3 can be approximated by multiplicative Hill functions, which are further approximated by multiplicative step functions [29]. Denoting u_{mancozeb} the mancozeb stress signal, the step function $s^+(u_{\text{mancozeb}}, \theta_{\text{mancozeb}})$ evaluates to 1(0) if mancozeb is (not) present. In Fig. 3 the synthesis rate of PDR3 is approximated by the following function

$$f_{\text{pdr3}}(x_{\text{yrr1}}, x_{x_{\text{yap1}}}, u_{\text{mancozeb}}) = \kappa^1_{\text{pdr3}} s^+(x_{\text{yrr1}}, \theta^1_{\text{yrr1}}) \times s^+(x_{\text{yap1}}, \theta^1_{\text{yap1}}) s^+(u_{\text{mancozeb}}, \theta_{\text{mancozeb}})$$

It expresses that PDR3 is synthesised at a rate κ^1_{pdr3}, if Yrr1 and Yap1 concentrations are above their threshold values and if mancozeb is present. We use the same step-function formulation with different threshold values of Yap1 and Yrr1 concentrations to describe the activation of FLR1 expression by the complex Yrr1 − Yap1*. Likewise, we describe the positive effect of Yap1* on gene expression by means of the step-function product $s^+(x_{\text{yap1}}, \theta_{\text{yap1}}) s^+(u_{\text{mancozeb}}, \theta_{\text{mancozeb}})$.

2.1.3 PL differential equations for the FLR1 network:

We combined the different step-function expressions describing the direct and indirect network interactions to obtain seven PL differential equations. As will be described below, this required formalising a number of experimental observations from [15] to describe the regulation of protein synthesis by the network proteins. Table 1 shows the final version of the model obtained after several iterations of the model building process. Initial versions of the model

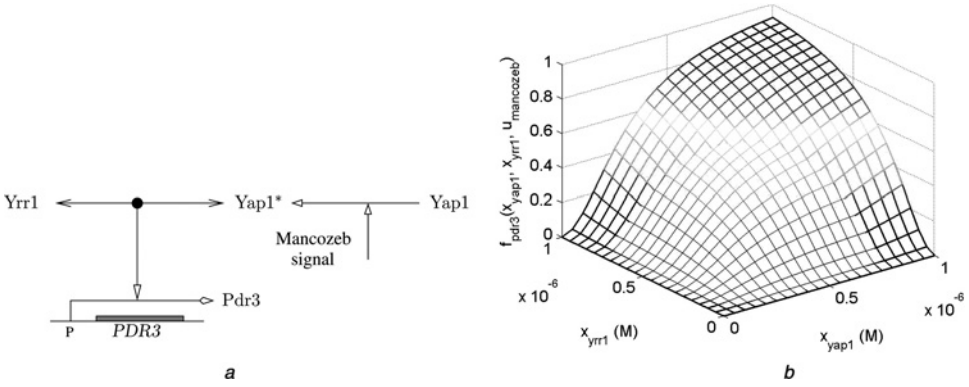

Fig. 3 *Transcriptional regulator activated by mancozeb*

a Regulation of PDR3 expression by the Yrr1 − Yap1* complex
b Activity of the PDR3 promoter as a function of Yrr1 and Yap1 concentrations in the presence of mancozeb

considered neither the direct influence of Pdr3 on FLR1 up-regulation, nor the inclusion of the new transcription factor FactorX meant to explain the additive effect of Yrr1 on YAP1 transcription (see single and double mutants in supplementary Tables 1 and 2, respectively).

2.1.3.1 FLR1: According to [15], three network proteins stimulate FLR1 transcription: Yap1, Yrr1 and Pdr3. In a Δyap1 single mutant, there is no FLR1 expression, while the single deletion of PDR3 and YRR1 results in a 2- and 3-fold decrease of FLR1 expression, respectively. We describe these effects by introducing three synthesis rates, κ^1_{flr1}, κ^2_{flr1} and κ^3_{flr1}, all modulated by Yap1* (see PL differential equation in Table 1). In the absence of the activated protein $(s^+(x_{yap1},\theta_{yap1}1)s^+(u_{mancozeb},\theta_{mancozeb}) = 0$ because either $x_{yap1} < \theta^1_{yap1}$ or $u_{mancozeb} < \theta_{mancozeb})$, FLR1 can only be expressed at a basal rate κ^b_{flr1}. This leads to a basal level of the FLR1 protein in yeast cells, given by the ratio $\kappa^b_{flr1}/\gamma_{flr1}$. The maximal level of FLR1, $(\kappa^b_{flr1} + \kappa^1_{flr1} + \kappa^2_{flr1} + \kappa^3_{flr1})/\gamma_{flr1}$, can be reached in the presence of Yap1*, but also Pdr3 and Yrr1. The latter proteins modulate the κ^2_{flr1} and κ^3_{flr1} synthesis rates, respectively.

We complement the FLR1 PL differential equation with parameter inequalities that express the relative strength of the different interactions regulating its expression (see Table 1). The intracellular function of FLR1 is the extrusion of toxic compounds such as mancozeb, which becomes more efficient as the different intracellular levels of the protein are reached.

2.1.3.2 Pdr3 and Rpn4: The model equations for Pdr3 and Rpn4 are very similar. The expression of Pdr3 and Rpn4 is activated by the complex Yrr1 − Yap1*: the deletion of either YRR1 or YAP1 prevents transcriptional activation of PDR3 and RPN4 upon mancozeb exposure [15]. In addition to the basal synthesis rates κ^b_{pdr3} and κ^b_{rpn4}, we introduce the synthesis rates κ^1_{pdr3} and κ^1_{rpn4}, which are modulated by the complex Yrr1 − Yap1* (Table 1). We define only one threshold value for Pdr3 and Rpn4, above which the two proteins are able to regulate the expression of other genes. Pdr3 and Rpn4 reach this level upon mancozeb exposure only, which implies the parameter inequalities of Table 1.

2.1.3.3 Yrr1: Upon mancozeb exposure, Yap1* acts at different levels on YRR1 expression, independently from the transcriptional activation by Pdr3 [15, 20]. We thus define three synthesis rates for Yrr1, two of them being modulated by Yap1* (κ^1_{yrr1} and κ^3_{yrr1}) and one by Pdr3 (κ^2_{yrr1}). In addition, we introduce three threshold concentrations: θ^1_{yrr1}, above which Yrr1 stimulates the expression of PDR3, RPN4 and FactorX; θ^2_{yrr1} for the activation of FLR1 expression; and θ^3_{yrr1} which is crossed when Yrr1 reaches its maximal level in the presence of high levels of Yap1* $((\kappa^b_{yrr1} + \kappa_{yrr1}1 + \kappa_{yrr1}2 + \kappa_{yrr1}3)/\gamma_{yrr1})$. This justifies the parameter inequalities for Yrr1 in Table 1.

Table 2 Corresponding domains in the phase space for the two existing attractors: basal steady state, without mancozeb-induced stress and response steady state, upon mancozeb-induced stress

Basal steady state	Response steady state
$x_{flr1} = \kappa^b_{flr1}/\gamma_{flr1}$	$x_{flr1} = (\kappa^b_{flr1} + \kappa^1_{flr1} + \kappa^2_{flr1} + \kappa^3_{flr1})/\gamma_{flr1}$
$x_{factorX} = \kappa^b_{factorX}/\gamma_{factorX}$	$x_{factorX} = (\kappa^b_{factorX} + \kappa^1_{factorX})/\gamma_{factorX}$
$0 \le u_{mancozeb} < \theta_{mancozeb}$	$\theta_{mancozeb} < u_{mancozeb} \le \max_{mancozeb}$
$x_{pdr3} = \kappa^b_{pdr3}/\gamma_{pdr3}$	$x_{pdr3} = (\kappa^b_{pdr3} + \kappa^1_{pdr3})/\gamma_{pdr3}$
$x_{rpn4} = \kappa^b_{rpn4}/\gamma_{rpn4}$	$x_{rpn4} = (\kappa^b_{rpn4} + \kappa^1_{rpn4})/\gamma_{rpn4}$
$x_{yap1} = \kappa^b_{yap1}/\gamma_{yap1}$	$x_{yap1} = (\kappa^b_{yap1} + \kappa^1_{yap1} + \kappa^2_{yap1} + \kappa^3_{yap1})/\gamma_{yap1}$
$x_{yrr1} = \kappa^b_{yrr1}/\gamma_{yrr1}$	$x_{yrr1} = (\kappa^b_{yrr1} + \kappa^1_{yrr1} + \kappa^2_{yrr1} + \kappa^3_{yrr1})/\gamma_{yrr1}$

2.1.3.4 Yap1: Two transcription factors stimulate YAP1 expression, Rpn4 and a still unknown transcription factor called FactorX, as well as the presence of mancozeb. They modulate the three synthesis rates, κ^1_{yap1} to κ^3_{yap1} (Table 1). This allows the intracellular level of Yap1 to progressively raise (see the parameter ordering in Table 1), from a threshold concentration θ^1_{yap1}, above which Yap1 stimulates the expression of most network genes, to θ^2_{yap1}, crossed when YAP1 expression is activated by Rpn4. It eventually reaches θ^3_{yap1}, above which Yap1 stimulates the expression of FLR1 and YRR1 genes. This threshold value is reached through the indirect activation of YAP1 by Yrr1, mediated by FactorX.

2.1.3.5 FactorX: FactorX was introduced based on discrepancies between results obtained with the first versions of the model and the experimental data acquired to test those predictions (see [15, 20]). The PL equation for this factor will be justified later: we have simply introduced a synthesis constant that can be modulated by Yrr1 in the presence of mancozeb ($\kappa^1_{factorX}$), in addition to a basal synthesis rate ($\kappa^b_{factorX}$). We define one threshold value for FactorX ($\theta^1_{factorX}$), above which the protein stimulates YAP1 transcription.

2.2 Analysis and verification of the FLR1 gene mancozeb response model

The state transition graph (STG) containing the model's dynamical behaviour consists of approximately 10^5 states. However, the FLR1 gene exhibits a low concentration level in the absence of mancozeb corresponding to the basal steady state. When considering the basal steady state as the initial condition, the STG still reaches a few hundred of states, which is still difficult to analyse purely by visual inspection. We have therefore recurred to formal methods for the analysis of these behaviours and for the identification and reachability of the attractors.

2.2.1 Identification and reachability of attractors: We identified two attractors in the STG (see Table 2). The existence of bistability is consistent with the fact that there is no negative interaction in the existing cycles in the FLR1 network. The first attractor is an asymptotically stable steady state of the PL model, identified as basal steady state in Table 2. It is characterised by a low expression of all the transcription factors and the FLR1 gene. This is consistent with the situation where the signal corresponding to the entry of mancozeb into the cytosol is absent, therefore not activating the network regulators and keeping FLR1 at a basal level. The second attractor corresponds to another asymptotically stable steady state of the PL model, identified as response steady state in Table 2. It is characterised by the presence of the mancozeb signal, which activates the cascade of regulators, leading to the stimulation of FLR1 expression.

We verified the reachability of each attractor by specifying two biological properties (temporal logic formulas 1 and 2 in Table 3) with the pattern-based property editor implemented

doi: 10.1049/iet-syb.2011.0001

in GNA. We fixed the initial conditions to the values corresponding to the basal steady state perturbed with a mancozeb stress signal ($u_{\text{mancozeb}} > \theta_{\text{mancozeb}}$). The formal verification analysis returned false (true) for the formula 1 (2), suggesting that the presence or absence of the mancozeb signal determines the reachability of each attractor.

This fact was confirmed by the specification of two additional biological properties (temporal logic formulas 3 and 4 in Table 3), where the presence (absence) of the mancozeb signal is denoted as sig_m ($\neg\text{sig}_m$). By considering the whole phase space for the initial conditions, the verification returned true for both properties. This indicates that the attractors are mutually exclusive and dependent on the presence of the mancozeb signal, which separates the phase space into two distinct STGs. This means that even though there is an absence of negative regulations in the interaction network (suggesting bistability), the proposed model of the FLR1 response to mancozeb presents a mancozeb-dependent monostable response.

2.2.2 Validation of cascade of activation: We verified if the model required full activation of the main regulators Yap1 and Yrr1 for the transcriptional activation of FLR1. We started by specifying a property to check for the existence of a path leading to a high concentration level of FLR1 before a high concentration level of Yap1 and Yrr1 (temporal logic formula 5 in Table 3). It considers the following protein concentration ranges Yap1_Yrr1_high_level ($x_{\text{yap1}} \geq \theta^3_{\text{yap1}} \wedge x_{\text{yrr1}} \geq \theta^3_{\text{yrr1}}$) and FLR1_high_level ($x_{\text{flr1}} \geq (\kappa^b_{\text{flr1}} + \kappa^1_{\text{flr1}} + \kappa^2_{\text{flr1}} + \kappa^3_{\text{flr1}})/\gamma_{\text{flr1}}$). Constraining the initial conditions to the basal steady state, the model checker returned false, indicating that the model cannot generate a path reaching a high concentration level of FLR1 without reaching first a high concentration level of Yap1 and Yrr1. This was confirmed through another property (temporal logic formula 6 of Table 3). This is consistent with the experimental data which shows the necessity of Yap1 and Yrr1 for the full activation of the FLR1 gene in the presence of mancozeb [15].

2.2.3 Pdr3 necessity for FLR1 maximum expression: As previously mentioned, the full activation of FLR1 is dependent on Yap1, Yrr1, Pdr3 and Rpn4 [15]. The effect of Yap1 and Yrr1 in FLR1 transcription is known to be direct [21, 22]. Rpn4-binding loci cannot be found in the FLR1 promoter region, so Rpn4 is assumed to influence FLR1 through Yap1, whose expression is dependent on Rpn4 in the presence of mancozeb [15]. We made the assumption that Pdr3 acts as co-transcription factor of Yrr1 when regulating FLR1, and we were interested in verifying if the model accounted for the fact that the full activation of FLR1 is dependent on Pdr3.

We started by specifying a property to check for the existence of a path leading to a high concentration level of FLR1 before a high concentration level of Pdr3 (temporal logic formula 7 of Table 3), considering the protein concentration range Pdr3_high_level ($x_{\text{pdr3}} > \theta^1_{\text{pdr3}}$). The model checker returned false, indicating that a high concentration level of FLR1 must be preceded by a high concentration level of Pdr3. This fact was reinforced by a second biological property (temporal logic formula 8 of Table 3), confirming that the maximal expression of FLR1 is dependent on its co-regulation by Pdr3 and Yrr1 transcription factors. This is consistent with the previous observation that site-directed mutagenesis of the predicted Pdr3 binding site in the FLR1 promoter reduces the level of mancozeb-induced activation of this gene [20].

2.2.4 Validation of a new Yap1 regulator: FactorX: The Δyrr1Δpdr3 double deletion mutant [20] exhibits YAP1 transcript levels coincident with those found in the Δyrr1 single-deletion mutant [15], suggesting that Pdr3 influence on the YAP1 up-regulation is dependent on Yrr1. Regarding the Rpn4 influence on YAP1 up-regulation, the double-deletion mutant Δyrr1Δrpn4 exhibits YAP1 transcript levels qualitatively lower than those observed for the single mutants Δyrr1 and Δrpn4, meaning that there is an additive effect of Yrr1 and Rpn4 in YAP1 up-regulation. Given that there is no previous evidence for a direct role of Yrr1 neither in YAP1 transcription nor in Yrr1 binding site in the YAP1 promoter region, the unknown transcription factor FactorX is proposed to mediate this interaction between Yrr1 and YAP1. Other examples can be found in the literature where putative variables are proposed to be included in the model, providing an explanation to the available biological data [32, 33].

In order to verify if the model accounted for the Yrr1 and Rpn4 additive effect, we considered two mutated models with ΔfactorXΔrpn4 and ΔfactorXΔyrr1 double knockouts (see Section 5), respectively. The response steady states identified for each of the mutated models (see supplementary Tables 1 and 2), indicate that in the absence of FactorX, a knockout of Rpn4 or Yrr1 severely hinders the concentration level of FLR1.

We then specified a biological property (temporal logic formula 9 of Table 3), to ensure the need of FactorX on the transcriptional activation of YAP1 in the absence of

Table 3 Biological properties used to validate the FLR1 gene mancozeb response model specified in temporal logic formulas

#	Temporal logic formula	Model-checker verdict
1	$\text{EF}(\text{attractor}_{\text{basal}})$	false
2	$\text{EF}(\text{attractor}_{\text{response}})$	true
3	$\text{AG}(\neg\ \text{sig}_m \Rightarrow \text{AF}(\text{attractor}_{\text{basal}}))$	true
4	$\text{AG}(\text{sig}_m \Rightarrow \text{AF}(\text{attractor}_{\text{response}}))$	true
5	E[(¬Yap1_Yrr1_high_level) ∪ FLR1_high_level]	false
6	EF(FLR1_high_level) ∧ ¬ *E*(¬Yap1_Yrr1_high_level ∪ FLR1_high_level)	true
7	E[(¬Pdr3_high_level) ∪ FLR1_high_level]	false
8	EF(FLR1_high_level) ∧ ¬ *E*(¬Pdr3_high_level ∪ FLR1_high_level)	true
9	*E*[(¬Rpn4_high_level) ∪ ¬Yap1_low_level] ∧ AG((¬Yap1_low_level ∧ ¬Rpn4_high_level) ⇒ FactorX_high_level)	true
10	AG(FLR1_high_level ⇒ FactorX_high_level)	true

Rpn4. Additionally, we considered another biological property (temporal logic formula 10 of Table 3), to verify that all the behaviours of the model leading to a high concentration level of FLR1 have a high concentration level of FactorX. We have considered the protein concentration ranges Yap1_low_level ($x_{yap1} \leq (\kappa^b_{yap1} + \kappa^1_{yap1})/\gamma_{yap1}$), FactorX_ high_level ($x_{factorX} > \theta^1_{factorX}$) and Rpn4_high_ level ($x_{rpn4} > \theta^1_{rpn4}$). The model checker returns true for both properties, confirming that in the proposed model high concentration levels of Yap1 and FactorX are essential for a full activation of FLR1. The identification of FactorX remains to be established.

3 Discussion

Some key regulators involved in the transcriptional activation of the FLR1 gene, in response to the induced stress, were previously identified [15, 20]. However, the lack of sufficient data on the kinetic parameter values and protein concentrations has hampered the study of the logic of the regulatory interactions. This has motivated the use of a qualitative approach based on a class of PL differential equations [27] using step functions for the description of the regulatory logic. Based on the available experimental data, the dynamical behaviour of the network was modelled using six coupled PL differential equations and 48 inequality constraints on the parameter values. A formal analysis of the model was performed using a recent version of GNA [25, 26], which includes a verification module allowing the transparent use of formal verification techniques.

Although the presented model takes only into account a handful of the FLR1 transcriptional regulators, it is already very useful to clarify that the maximal expression of the FLR1 gene is achieved through the co-regulation of Pdr3 and Yrr1 transcription factors. The observation that the double-deletion mutant Δyrr1Δrpn4 exhibits YAP1 transcript levels qualitatively lower than those observed for the single mutants Δyrr1 and Δrpn4 led us to the identification of the Yrr1 and Rpn4 additive effect [20]. Given that there is also no previous evidence for a direct role of neither Yrr1 in YAP1 transcription nor Yrr1 binding site in the YAP1 promoter region, we introduced a new transcription factor FactorX to account for the interaction between Yrr1 and YAP1. We have also assessed the robustness of the model, by performing single and double knockouts (see supplementary Tables 1 and 2) and changing the ordering of the parameters (see supplementary Table 3). This analysis enabled us to confirm the critical importance of Yap1 and Yrr1 for the reachability of the response steady state. Additionally, through the temporal logic formulas 9 and 10, we ensured that the regulatory influence of FactorX was essential for the generation of the additive effect of Yrr1 and Rpn4 on Yap1.

Despite the importance of the results and the good fit to real data, there are certain phenomena that are not taken into account by this model like, for example, the transport of the transcription factors from the cytoplasm, where they are synthesised, to the nucleus, where they regulate gene expression. Such phenomena may introduce delays that can account for some differences between the experimental data and the model predictions, since the experimental data used in this study concern mRNA and not protein levels.

In the previous study [20], the network was manually built, by taking into consideration the available biological data. There are, however, some methods that could be used for the identification of the regulatory interactions (see [34] as an example) in genetic regulatory networks from gene expression data. An interesting future work would be to compare the considered network with networks built by such methods.

4 Conclusions

In summary, we have built a model for the genetic regulatory network controlling FLR1 up-regulation in response to mancozeb stress in *S. cerevisiae*. We have specified the available biological data in temporal logic formulas and verified the behaviours generated by the model. By performing single and double knockouts, as well as by changing the order of the parameters (see supplementary Tables 1–3), we tested the network robustness to perturbations along the cascade of activation. In particular, the comparison between the experimental data and the predicted steady states in the wild-type strain, as well as in the corresponding single and double mutants, confirmed the necessity to consider a new transcription factor to mediate the interaction between Yrr1 and the expression levels of Yap1. The inclusion of this new transcription factor in the network reinforces the usefulness of having a model to quickly formulate new hypotheses. Also, the advantage of the model extends to the easiness of performing new analyses with single or double mutants in a reliable and cost-effective manner.

5 Methods

5.1 Modelling of network interactions by means of step functions

In this section, we describe the kinetic models that were developed to describe the control of gene expression by transcriptional regulators.

5.1.1 Transcriptional activator: We consider the case of YAP1 activation by the transcription factor Rpn4. We describe the regulation by means of the sigmoidal Hill function, which relates the activity of a given gene with the concentration of its transcriptional regulator

$$f_{yap1}(x_{rpn4}) = \frac{x_{rpn4}^{n_{rpn4}}}{x_{rpn4}^{n_{rpn4}} + K_{rpn4}^{n_{rpn4}}}$$

where $n_{rpn4} > 1$ is the cooperativity coefficient and K_{rpn4} an apparent dissociation constant. Even though we ignore the precise values of the parameters, we use reasonable estimates and obtain the plot in Fig. 2*b* ($K_{rpn4} = 3 \times 10^{-7} M$ and $n_{rpn4} = 2$).

5.1.2 Transcriptional activator activated by mancozeb: Following the same line of reasoning, we can describe the activity of the PDR3 promoter by means of the following Hill function

$$f_{pdr3}(x_{yrr1}, x_{x_{yap1}}, u_{mancozeb}) = \frac{x_C^{n_C}}{x_C^{n_C} + K_C^{n_C}}$$

where x_C is the concentration of the Yrr1 − Yap1* complex, K_C a dissociation constant and n_C the cooperativity number. In order to establish a step-function expression for PDR3

doi: 10.1049/iet-syb.2011.0001

promoter activity, we need to model the complex formation following mancozeb exposure.

The reactions leading to the formation of the Yrr1 − Yap1* complex are shown in Fig. 2*a*. They can be described by the following ODEs

$$\dot{x}_{\text{yap1*}\sim} = k_1 x_{\text{yap1}\sim} h^+(u_{\text{mancozeb}}, u_{\text{mancozeb}}, n_{\text{mancozeb}}) - \gamma_{\text{yap1*}} x_{\text{yap1*}\sim} - k_2 x_{\text{yap1*}\sim} x_{\text{yrr1}\sim} + k_3 x_C$$

$$\dot{x}_C = k_2 x_{\text{yap1*}\sim} x_{\text{yrr1}\sim} - k_3 x_C$$

where $x_{\text{yap1*}\sim}$ and $x_{\text{yrr1}\sim}$ denote the free concentrations of Yap1* and Yrr1, k_1 is the rate constant for the activation of Yap1, and k_2 and k_3, the forward and reverse constants for Yrr1 − Yap1* formation.

The following conservation relations holds for $x_{\text{yap1*}}$ and x_{yrr1}

$$x_{\text{yap1*}} = x_{\text{yap1*}\sim} + x_C$$

$$x_{\text{yrr1}} = x_{\text{yrr1}\sim} + x_C$$

We use these relations to formulate the differential equations for the total Yr11 and Yap1* concentrations

$$\dot{x}_{\text{yap1*}} = k_1 x_{\text{yap1}} h^+(u_{\text{mancozeb}}, u_{\text{mancozeb}}, n_{\text{mancozeb}}) - \gamma_{\text{yap1*}} x_{\text{yap1*}}$$

$$\dot{x}_C = k_2 (x_{\text{yap1*}} - x_C)(x_{\text{yrr1}} - x_C) - k_3 x_C$$

We apply a quasi-steady-state approximation for Yap1 activation and a rapid-equilibrium assumption for the complex formation, because these two processes take place in a much faster time scale than protein synthesis and degradation. This yields the following expression for the complex concentration

$$x_C = \frac{k_1 h^+(u_{\text{mancozeb}}, u_{\text{mancozeb}}, n_{\text{mancozeb}}) x_{\text{yap1}} x_{\text{yrr1}}}{K_2 \gamma_{E1*}}$$

with $K_2 = k_3/k_2$. With this algebraic expression, we can now compute PDR3 promoter activity $f_{\text{pdr3}}(x_{\text{yrr1}}, x_{x_{\text{yap1}}, u_{\text{mancozeb}}})$ ($K_2 = 10^{-7}M$, $k_1 = 0.1386\text{min}^{-1}$, $K_C = 3.5 \times 10^{-5}M$, $n_C = 2$). In the absence of mancozeb ($h^+(u_{\text{mancozeb}}, u_{\text{mancozeb}}, n_{\text{mancozeb}}) = 0$), the complex is not formed and the promoter activity is null. In the presence of drug ($h^+(u_{\text{mancozeb}}, u_{\text{mancozeb}}, n_{\text{mancozeb}}) \simeq 1$), the activity of the promoter is a sigmoidal surface, which depends on both Yap1 and Yrr1 concentrations (Fig. 3).

The surface can be approximated by fitting a multiplicative expression of Hill functions, where θ_{yap1} and θ_{yrr1} are threshold concentrations, and n_{yap1} and n_{yrr1} cooperativity constants

$$f_{\text{pdr3}}(x_{\text{yrr1}}, x_{x_{\text{yap1}}}, u_{\text{mancozeb}}) \simeq h^+(x_{\text{yrr1}}, \theta_{\text{yrr1}}, n_{\text{yrr1}}) \times h^+(x_{\text{yap1}}, \theta_{\text{yap1}}, n_{\text{yap1}}) h^+(u_{\text{mancozeb}}, u_{\text{mancozeb}}, n_{\text{mancozeb}})$$

The Hill functions are then approximated by step functions, which yields the following expression to describe PDR3 activation by Yrr1 − Yap1*: $s^+(x_{\text{yrr1}}, \theta_{\text{yrr1}}1) s^+(x_{\text{yap1}}, \theta_{\text{yap1}}1) s^+(u_{\text{mancozeb}}, \theta_{\text{mancozeb}})$.

5.2 Formal analysis and verification of qualitative models using GNA

GNA [26] implements the PL mathematical framework through a discretisation of the continuous dynamics, resulting in a STG, that is, a graph structure containing all the possible behaviours of a system, where the nodes represent the states of the system and the edges the possible transitions between the states. This STG can be visualised and the characteristics of the states inspected.

Upon complete definition of the PL system, the identification and classification of the PL system steady states can be performed using the attractor search functionality available in GNA [35]. It uses a SAT-based approach avoiding the generation of the whole STG through simulation. Throughout the iterative process of modelling, it simplifies the identification of the model attractors, as well as the assessment of the impact of single and double knockouts on these attractors. A Δvar knockout in the model corresponds to a restriction of the value of variable var to zero. Since we are modelling the activation of the regulatory cascade upon mancozeb stress (i.e. presence of mancozeb signal), we achieved this by adding a step function $s^-(u_{\text{mancozeb}}, \theta_{\text{mancozeb}})$ to all the synthesis rates of variable var, which is always evaluated to zero.

The use of model checking technology is performed through the verification model of GNA [25], where the biological properties are specified as statements in temporal logic (presented in Table 3), using the available pattern-based property editor [36]. The verification result is composed of a true (false) verdict together with a witness (counterexample) supporting the verdict. The variable evolution throughout the states composing this witness/counterexample can also be visualised [25].

6 Acknowledgments

This work was partially supported by the FCT program (PhD grant SFRH/BD/32965/2006 and SFRH/BD/23331/2005 to PTM and PJD, respectively) and the PDTC program (project PTDC/EIA/71587/2006 and PTDC/BIO/72063/2006). The authors are also thankful to the anonymous reviewers for their useful comments and suggestions.

7 References

1 Gilbert, D., Heiner, M., Lehrack, S.: 'A unifying framework for modelling and analysing biochemical pathways using Petri nets' (*LNBI*, **4695**), Proc. Fifth Conf. Computational Methods in Systems Biology (CMSB 2007), pp. 200–216

2 Antoniotti, M., Policriti, A., Ugel, N., Mishra, B.: 'Model building and model checking for biochemical processes', *Cell Biochem. Biophys.*, 2003, **38**, (3), pp. 271–286

3 Batt, G., Ropers, D., de Jong, H., *et al.*: 'Validation of qualitative models of genetic regulatory networks by model checking: analysis of the nutritional stress response in *Escherichia coli*', *Bioinformatics*, 2005, **21**, (Suppl. 1), pp. i19–i28

4 Batt, G., Yordanov, B., Belta, C., Weiss, R.: 'Robustness analysis and tuning of synthetic gene networks', *Bioinformatics*, 2007, **23**, (18), pp. 2415–2422

5 Bernot, G., Comet, J.P., Richard, A., Guespin, J.: 'Application of formal methods to biological regulatory networks: extending Thomas' asynchronous logical approach with temporal logic', *J. Theor. Biol.*, 2004, **229**, (3), pp. 339–348

6 Calder, M., Vyshemirsky, V., Gilbert, D., Orton, R.: 'Analysis of signalling pathways using the PRISM model checker', Proc. Third Conf. Computational Methods in Systems Biology (CMSB 2005), 2005, pp. 79–90

7 Chabrier-Rivier, N., Chiaverini, M., Danos, V., Fages, F., Schächter, V.: 'Modeling and querying biomolecular interaction networks', *Theor. Comput. Sci.*, 2004, **325**, pp. 25–44

8 Fisher, J., Piterman, N., Hajnal, A., Henzinger, T.: 'Predictive modeling of signaling crosstalk during *C. elegans* vulval development', *PLoS Comput. Biol.*, 2007, **3**, (5), p. e92

9 Shen, X., Collier, J., Dill, D., Shapiro, L., Horowitz, M., Mcadams, H.: 'Architecture and inherent robustness of a bacterial cell-cycle control system', *Proc. Natl. Acad. Sci. USA*, 2008, **105**, (32), pp. 11340–11345

10 Thomas, R.: 'Logical analysis of systems comprising feedback loops', *J. Theor. Biol.*, 1978, **73**, pp. 631–656

11 Li, F., Long, T., Lu, Y., Ouyang, Q., Tang, C.: 'The yeast cell-cycle network is robustly designed', *Proc. Natl. Acad. Sci. USA*, 2004, **101**, (14), pp. 4781–4786

12 Shmulevich, I., Dougherty, E., Kim, S., Zhang, W.: 'Probabilistic Boolean networks: a rule-based uncertainty model for gene regulatory networks', *Bioinformatics*, 2002, **18**, (2), pp. 261–274

13 Koch, I., Junker, B., Heiner, M.: 'Application of Petri net theory for modelling and validation of the sucrose breakdown pathway in the potato tuber', *Bioinformatics*, 2005, **21**, (7), pp. 1219–1226

14 Chaouiya, C., Remy, E., Thieffry, D.: 'Qualitative Petri net modelling of genetic networks', in Istrail, S., Pevzner, P., Waterman, M. (Eds.): 'Transactions on computational systems biology VI (*LNCS*, **4220**)', (Springer, Berlin, 2006), pp. 95–112

15 Teixeira, M., Dias, P., Simoes, T., Sá-Correia, I.: 'Yeast adaptation to mancozeb involves the up-regulation of FLR1 under the coordinate control of Yap1, Rpn4, Pdr3, and Yrr1', *Biochem. Biophys. Res. Commun.*, 2008, **367**, (2), pp. 249–255

16 Brôco, N., Tenreiro, S., Viegas, C., Sá-Correia, I.: 'FLR1 gene (ORF YBR008c) is required for benomyl and methotrexate resistance in *Saccharomyces cerevisiae* and its benomyl-induced expression is dependent on Pdr3 transcriptional regulator', *Yeast*, 1999, **15**, pp. 1595–1608

17 Nguyen, D., Alarco, A., Raymond, M.: 'Multiple Yap1p-binding sites mediate induction of the yeast major facilitator FLR1 gene in response to drugs, oxidants, and alkylating agents', *J. Biol. Chem.*, 2001, **276**, pp. 1138–1145

18 Tenreiro, S., Fernandes, A., Sá-Correia, I.: 'Transcriptional activation of FLR1 gene during *Saccharomyces cerevisiae* adaptation to growth with benomyl: role of Yap1p and Pdr3p', *Biochem. Biophys. Res. Commun.*, 2001, **280**, pp. 216–222

19 Cabrito, T., Teixeira, M., Sá-Correia, I.: 'Global adaptive response and resistance to agricultural fungicides: lessons from yeast and phytopathogenic fungi', in Costa, P.D., Bezerra, P. (Eds.): 'Fungicides: chemistry, environmental impact and health effects' (Nova Science Publishers, New York, USA, 2009), pp. 228–253

20 Teixeira, M., Dias, P., Monteiro, P., *et al.*: 'Refining current knowledge on the yeast FLR1 regulatory network by combined experimental and computational approaches', *Mol. Biosyst.*, 2010, **6**, (12), pp. 2471–2481

21 Lucau-Danila, A., Lelandais, G., Kozovska, Z., *et al.*: 'Early expression of yeast genes affected by chemical stress', *Mol. Cell. Biol.*, 2005, **25**, (5), pp. 1860–1868

22 Le Crom, S., Devaux, F., Marc, P., Zhang, X., Moye-Rowley, W., Jacq, C.: 'New insights into the pleiotropic drug resistance network from genome-wide characterization of the YRR1 transcription factor regulation system', *Mol. Cell. Biol.*, 2002, **22**, (8), pp. 2642–2649

23 Fisher, J., Henzinger, T.: 'Executable cell biology', *Nat. Biotechnol.*, 2007, **25**, (11), pp. 1239–1250

24 Clarke, E., Grumberg, O., Peled, D.: 'Model checking' (MIT Press, 2000)

25 Monteiro, P., Dumas, E., Besson, B., *et al.*: 'A service-oriented architecture for integrating the modeling and formal verification of genetic regulatory networks', *BMC Bioinformatics*, 2009, **10**, p. 450

26 de Jong, H., Geiselmann, J., Hernandez, C., Page, M.: 'Genetic network analyzer: qualitative simulation of genetic regulatory networks', *Bioinformatics*, 2003, **19**, (3), pp. 336–344

27 Glass, L., Kauffman, S.: 'The logical analysis of continuous non-linear biochemical control networks', *J. Theor. Biol.*, 1973, **39**, pp. 103–129

28 Chaves, M., Sontag, E., Albert, R.: 'Methods of robustness analysis for Boolean models of gene control networks', *Syst. Biol. (Stevenage)*, 2006, **153**, (4), pp. 154–167

29 Ropers, D., Baldazzi, V., de Jong, H.: 'Model reduction using piecewise-linear approximations preserves dynamic properties of the carbon starvation response in Escherichia coli', *IEEE/ACM Trans. Comput. Biol. Bioinform.*, 2011, **8**, pp. 166–181

30 Cantone, I., Marucci, L., Iorio, F., *et al.*: 'A yeast synthetic network for in vivo assessment of reverse-engineering and modeling approaches', *Cell*, 2009, **137**, pp. 172–181

31 Azevedo, D., Tacnet, F., Delaunay, A., Rodrigues-Pousada, C., Toledano, M.: 'Two redox centers within Yap1 for H_2O_2 and thiol-reactive chemicals signaling', *Free Radic. Biol. Med.*, 2003, **35**, (8), pp. 889–900

32 Locke, J., Southern, M., Kozma-Bognár, L., *et al.*: 'Extension of a genetic network model by iterative experimentation and mathematical analysis', *Mol. Syst. Biol.*, 2005, **1**, article no: 2005.0013

33 Rubinstein, A., Gurevich, V., Kasulin-Boneh, Z., Pnueli, L., Kassir, Y., Pinter, R.Y.: 'Faithful modeling of transient expression and its application to elucidating negative feedback regulation', *Proc. Natl. Acad. Sci. USA*, 2007, **104**, (15), pp. 6241–6246

34 Drulhe, S.: 'Identification of genetic regulatory networks from gene expression data: an approach based on piecewise-affine models'. PhD thesis, Université Joseph Fourier – Grenoble I, 2008

35 de Jong, H., Page, M.: 'Search for steady states of piecewise-linear differential equation models of genetic regulatory networks', *ACM/IEEE Trans. Comput. Biol. Bioinform.*, 2008, **5**, (2), pp. 508–522

36 Monteiro, P., Ropers, D., Mateescu, R., Freitas, A., de Jong, H.: 'Temporal logic patterns for querying dynamic models of cellular interaction networks', *Bioinformatics*, 2008, **24**, (16), pp. i227–i233

doi: 10.1049/iet-syb.2011.0001